International Journal of High-Rise Buildings
Vol 1, No 2, June 2012, 87-97

International Journal of
High-Rise Buildings
www.ctbuh.org

Analysis of Airflow Pattern and Particle Dispersion in Enclosed Environment Using Traditional CFD and Lattice Boltzmann Methods

Tomo Inoguchi and Kazuhide Ito†

Interdisciplinary Graduate School of Engineering Science, Kyushu University, Fukuoka, 816-8580, Japan

Abstract

The indoor environments in high-rise buildings are generally well enclosed by defined boundary conditions. Here, a numerical simulation method based on the Lattice Boltzmann method (LBM), which aims to model and simulate the turbulent flow accurately in an enclosed environment, and its comparison with traditional computational fluid dynamics (CFD) results, are presented in this paper. CFD has become a powerful tool for predicting and evaluating enclosed airflows with the rapid advance in computer capacity and speed, and various types of CFD turbulence modeling and its application and validation have been reported. The LBM is a relatively new method; it involves solving of the discrete Boltzmann equation to simulate the fluid flow with a collision model instead of solving Navier-Stokes equations. In this study, the LBM-based scheme of flow pattern and particle dispersion analyses are validated using the benchmark test case of two- and three-dimensional and isothermal conditions (IEA/Annex 20 case); the prediction accuracy and advantages are also discussed by comparison with the results of CFD.

Keywords: Lattice Boltzmann method, Computational fluid dynamics, Enclosed environment, Particle dispersion, Benchmark test

1. Introduction

The indoor environments in high-rise buildings are generally well enclosed and insulated; accordingly, they are designed with mechanical ventilation systems to maintain a minimum outdoor airflow rate. In other words, the characteristics of a room in a high-rise building are enclosed by defined boundary conditions, for example, concrete geometry of the room, wall surface treatment and locations of supply/exhaust openings, especially in the design stage. The control of environmental quality is very important for maintaining the health and comfort of residents in a room as a convenient and enclosed space. The indoor airflow pattern and distributions of environmental parameters, for example, temperature, humidity and contaminants, are crucial and have a large impact on indoor air quality (IAQ) and thermal comfort; hence, numerical prediction methods of these have played an important role in evaluating and improving indoor environmental quality, especially in the design stage. The computational fluid dynamics (CFD) technique has become an increasingly useful tool for prediction of indoor airflow since the early 1970s because of the development in not only hardware but also software. The CFD has been applied in indoor environmental design with considerable success in recent decades (Nielsen et al., 2007).

The CFD approaches are normally classified into three stages: direct numerical simulation (DNS), Reynolds averaged Navier-Stokes (RANS) equation modeling, and large eddy simulation (LES).

DNS solves the highly reliable Navier-Stokes equations without approximations and hence DNS requires a grid resolution as fine as the Kolmogorov micro-scale. This is numerically very expensive, and it has thus been limited to low Reynolds number flows until now. Even now, the computer capacity is still far too small and DNS cannot be used to study typical indoor environments under realistic conditions, such as flow field analysis around and inside high-rise buildings.

The RANS approach solves ensemble-averaged Navier-Stokes equations by using turbulence modeling. RANS models can be classified into two groups: turbulent viscosity models and Reynolds-stress models. In the turbulent viscosity models, the standard k-ε model developed by Launder and Spalding is widely used in indoor environmental analysis and various kinds of modified model have been proposed and applied, including low Reynolds number-type models (Launder and Spalding, 1972). The Reynolds-stress models solve the transport equations for the Reynolds stresses. Generally, the performance of

†Corresponding author: Kazuhide Ito
Tel: +81-92-583-7628; Fax: +81-92-583-7627
E-mail: ito@kyudai.jp

Reynolds-stress models has not been much better than that of the Standard k-ε model, and weak points of these models are mathematical complexity and numerical instability (Zhai et al., 2007).

LES solves the large-eddy motion by a set of filtered equations governing the three-dimensional, time-dependent motion. Turbulent transport approximations are used for small eddies, which are modeled independently from the flow geometry. LES is clearly superior to RANS where the transport terms (e.g. Reynolds stresses) are treated with full empiricism. LES is also more realistic than DNS in engineering applications of CFD.

On the other hand, over the past two decades, the Lattice Boltzmann method (LBM) was developed into an efficient computational fluid dynamics tool. The LBM intrinsically possesses the essential microscopic physics ingredients and is well suited for handling more general boundary conditions owing to its kinetic nature. Recently, because of its simplicity of programming and capability of simulating complex fluid systems, LBM has rapidly emerged as a useful technique with great potential for numerically solving momentum, energy, species transport and multi-phase problems (Chen and Doolen, 1998).

In this paper, a numerical simulation method based on the LBM, which aims to model and simulate the turbulent flow and particle dispersion in an enclosed environment accurately, is presented and validated using the benchmark test case of two- and three-dimensional and isothermal conditions called the IEA/Annex 20 benchmark test case (Lemaire et al., 1993); its prediction accuracy and advantages are discussed by comparison with the results of RANS and LES as a traditional CFD approach.

Furthermore, contamination by aerosol particles indoors has now been identified and its serious health impact on residents of a building has been raised as a concern. In this study, particle dispersion characteristics in an enclosed space are analyzed by a Lagrangian approach based on steady flow pattern data predicted by RANS and LBM as examples of applied analysis; the prediction results are also discussed qualitatively.

2. Outline of Lattice Boltzmann Method (LBM)

The Lattice Boltzmann method (LBM) is a mesoscopic kinetic-based approach that assumes the fluid flow to be composed of a collision of pseudo-particles represented by a distribution function. On the other hand, the traditional CFD methods solve the conservation equations, for example, mass conservation, momentum conservation, energy and other scalar conservations of macroscopic properties.

The LBM was developed from the method of lattice gas automata (Frisch et al., 1986). It is a relatively new numerical scheme developed since the late 1990s. Nevertheless, this methodology has attracted much interest in many engineering fields recently. Compared with conventional computational fluid dynamics (CFD), it exhibits unique advantages in simulating fluid flows and associated transport phenomena, such as the ability to handle complicated boundary geometries, inherent parallelism, simplicity of programming, and memory efficiency (Grunau et al., 1993; Yu et al., 2003; Zhang et al., 2006).

2.1. Lattice BGK equation for velocity field

The LMB could be interpreted as the finite discrete velocity model of the Boltzmann equation. The pseudo-fluid particles are represented by the single-particle distribution function f_i. This is a function of node x and time t with velocity u_i. In this study, the lattice Boltzmann Bhatnagar-Gross-Krook model, hereafter, the BGK model, is used as a model that represents the change in distribution function of pseudo-fluid particles by collision (Bhatnagar et al., 1954). The particle distribution function satisfies the following lattice BGK equation. Here, high *Kn* (Knudsen number) but low *Ma* (Mach number) conditions are assumed.

$$f_i(\vec{x}+\vec{c}_i\Delta t, t+\Delta t) = f_i(\vec{x},t) - \frac{\Delta t}{\tau}(f_i(\vec{x},t) - f_i^{eq}(\vec{x},t)) + F_i(\vec{x},t) \quad (1)$$

Here, f_i is the particle velocity distribution function, τ is the non-dimensional relaxation time and Δt is time step, c_i represents the particle velocity in the discretized direction i, and x_i denotes space coordinate. F_i denotes an additional contribution of body force term and is disregarded in this study. f_i^{eq} is the local equilibrium distribution, and the following expression estimated by the method of Taylor expansion of Maxwell distribution of pseudo-particles under a thermodynamic equilibrium state is adopted.

$$f_i^{ep} = \rho w_i \left[1 + b\frac{\vec{c}_i\vec{u}}{c^2} + e\frac{u^2}{c^2} + h\frac{(\vec{c}_i\vec{u})^2}{c^4} \right] \quad (2)$$

Here, ρ is density, $c = \Delta x/\Delta t$, w_i is the weight factor (weight distribution) corresponding to the particle velocity vector, and u is the macroscopic velocity. In the case of the D2Q9 model (two-dimensional and nine velocities), undetermined coefficients in Eq. (2) are defined as follows:

$$f_i^{ep} = \rho w_i \left[1 + 3\frac{\vec{c}_i\vec{u}}{c^2} + \frac{3}{2}\frac{u^2}{c^2} + \frac{9}{2}\frac{(\vec{c}_i\vec{u})^2}{c^4} \right] \quad (3)$$

The macroscopic density of fluid $\rho(\vec{x},t)$ and momentum $\rho(\vec{x},t)\,u(\vec{x},t)$ are estimated as follows:

$$\rho(\vec{x},t) = \sum_i f_i(\vec{x},t) \quad (4)$$

$$\rho(\vec{x},t)u(\vec{x},t) = \sum_i f_i(\vec{x},t)c_i \quad (5)$$

The relaxation time is related to the viscosity and

expressed as follows:

$$\nu=\left(\tau-\frac{\Delta t}{2}\right)\theta \tag{6}$$

After the selection of appropriate lattice size and the characteristic velocity scale for LBM, the viscosity ν is calculated by the given Reynolds number (*Re*) and consequently the relaxation time τ is determined.

The LBM is discretized explicitly and can be coded by a simple algorithm. The LBM is an effective approach for unsteady fluid analysis that is appropriate for massively parallel computation.

2.2. Incorporation of turbulence model

Concerning the simulation of indoor environmental problems, large and complicated geometry of the target space and hence a wide-ranging Reynolds number flow are generally assumed. A relatively large computational domain will be required and subsequently the lattice size will become larger than the energy dissipation scale. From this point of view, it is necessary to introduce a turbulence model into the LBM scheme. In this paper, simple turbulence modeling using turbulent kinetic energy *k* and the effective turbulent relaxation time (time scale of local turbulent motion) τ_{eddy} (~k/ε) is incorporated.

$$\nu+\nu_{eddy}=\left(\tau-\frac{\Delta t}{2}\right)\theta \tag{7}$$

$$\nu_{eddy}=C_\mu k\tau_{eddy} \tag{8}$$

$$\tau_{eddy}=\Psi\left(\frac{k}{\varepsilon}\right) \tag{9}$$

Here, *k* is the turbulent kinetic energy, ε is the dissipation rate, and S is a measure of the local velocity gradient.

2.3. Wall treatment as boundary condition

All of the no-slip boundary condition for a fluid field is handled by the half-way bounce-back scheme (He et al., 1997). This kind of modified bounce-back scheme is of second-order spatial accuracy. The lattice distribution functions that will stream to no-slip boundary are reversed and then bounce back to the fluid field in the propagation process.

3. Outline of Traditional CFD

In order to validate the prediction results of the LBM-based scheme, numerical simulation with RANS model and LES as traditional CFD simulations is carried out. Here, standard k-ε model and a low Reynolds number-type k-ε model (Abe-Nagano-Kondo model) as RANS model and LES (Smagorinsky-Lilly model) are adopted.

3.1. Standard k-ε model

Standard k-ε model was proposed by Launder and Spalding (Launder and Spalding, 1972) and has been widely used for industrial and engineering applications of CFD because of its robustness, economy and reasonable accuracy for a wide range of turbulent flows. This is a semi-empirical model based on model transport equations for the turbulent kinetic energy *k* and its dissipation rate ε. The transport equation for *k* is derived from the exact equation, while the model transport equation for ε was obtained using physical reasoning and bears little resemblance to its mathematically exact counterpart. Turbulent kinematic viscosity ν_t is expressed by using *k* and ε as follows.

$$\nu_t=C_\mu\cdot\frac{k^2}{\varepsilon} \tag{10}$$

As the strengths and weaknesses of the Standard k-ε model have been validated and become known, modifications have been introduced to improve its prediction performance.

3.2. Low Reynolds number-type k-ε models

A lot of low Reynolds number-type k-ε models have been proposed since the 1970s and the Abe-Nagano-Kondo model successfully concluded that this approach can be applicable to a flow field with separation and reattachment and can actually predict back-step flow with high accuracy (Abe et al., 1992). The turbulent modeling of the Abe-Nagano-Kondo model in turbulent kinetic viscosity and damping function incorporating Kolmogorov length scale η and Kolmogorov velocity scale u_ε are expressed as follows:

$$\nu_t=C_\mu\cdot f_\mu\cdot\frac{k^2}{\varepsilon} \tag{11}$$

$$f_\mu=\left\{1-\exp\left(-\frac{y^*}{14}\right)\right\}\left[1+\frac{5}{R_t^{3/4}}\cdot\exp\left\{\left(\frac{R_t}{200}\right)^2\right\}\right] \tag{12}$$

$$R_t=\frac{k^2}{\nu\varepsilon},\ y^*=\frac{u_\tau y}{\nu}=\frac{y}{\eta},\ \eta=\frac{\nu^{3/4}}{\varepsilon^{1/4}},\ u_\varepsilon=(\nu\varepsilon)^{1/4} \tag{13}$$

3.3. Large eddy simulation

LES is an intermediate modeling technique between DNS and RANS. LES solves filtered Navier-Stokes equations for large-scale eddies while modeling small-scale, that is, subgrid-scale, eddies. Filtering of various variables in the Navier-Stokes equations is similar to the process of Reynolds averaging, and the resulting equations for incompressible flow can be written in a form similar to the RANS equations. Smagorinsky proposed the first subgrid model correlating eddy viscosity to the strain rate, which can be written in the form of eddy viscosity as follows (Smagorinsky, 1963):

$$\tau_{ij}=\frac{1}{3}\tau_{kk}\delta_{ij}-2\nu_{SGS}\overline{S}_{ij} \tag{14}$$

$$\nu_{SGS} = (C_s\overline{\Delta})^2 \cdot (2\overline{S}_{ij}\overline{S}_{ij})^{1/2} = (C_s\overline{\Delta})^2 |\overline{S}| \quad (15)$$

Here, $|\overline{S}| = (2\overline{S}_{ij}\overline{S}_{ij})^{1/2}$, is the filter width, and C_s is the Smagorinsky constant. Concerning the Smagorinsky constant C_s, Lilly suggested a value of 0.17 in homogeneous isotropic turbulent flow (Lilly, 1966) and Mizutani et al. suggested $C_s = 0.16$ for typical indoor airflow (Mizutani et al., 1991).

4. Target Benchmark Case

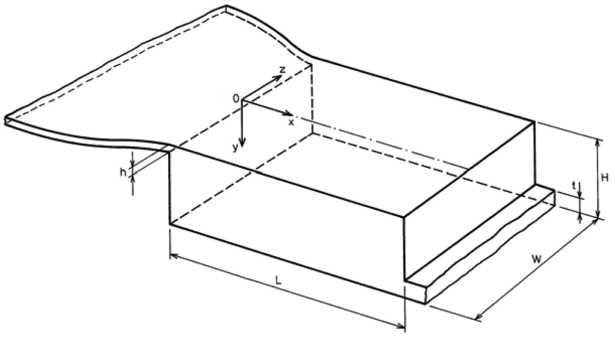
The model geometry of the benchmark test case is shown in Fig. 1. This model case has specifications of $H = 3.0$ m, $L = 9.0$ m, $h = 0.168$ m, and $t = 0.48$ m. W = 3.0 m was used for three-dimensional calculation. The height of the supply inlet opening is rather small compared with the exhaust outlet opening. The inlet condition for velocity U_{in} is 0.455 m/s and corresponds to Re = 5000 (= $U_{in}h/\nu$). The turbulence intensity of the inlet is 4%. The velocity distributions in this model were measured by laser-Doppler anemometry.

This benchmark test of flow in a room with a slot inlet called the "IEA 2D test case" was defined in 1992 to be used in the IEA Annex 20 work; there have been a very large number of papers that describe this geometry in other CFD work. The detailed information of the IEA 2D test case is reported elsewhere (Lemaire et al. 1993).

5. Cases Analyzed

In this study, prediction performance of flow pattern in an enclosed space by an LBM-based scheme is validated by using traditional CFD simulation results, and then particle dispersion analysis is carried out.

Two-dimensional flow field analyses by RANS model (Standard k-ε model and low Re-type k-ε model) and LBM are carried out in accordance with the geometry and boundary conditions in the IEA 2D test case. Three-dimensional flow field analyses by RANS model (Standard k-ε model and low Re-type k-ε model), LES (Smagorinsky-Lilly model) and LBM are also conducted in three-dimensional geometry of the IEA benchmark test case shown in Fig. 1.



$h/H = 0.056$, $L/H = 3.0$, $t/H = 0.16$

Figure 1. The model of the benchmark test case proposed by IEA Annex 20 (Lemaire et al. 1993).

Concerning particle dispersion analysis, Lagrangian-based particle tracking is conducted subsequently on the basis of the steady flow field data-estimated RANS model (Standard k-ε model and low Re-type k-ε model) and LBM.

6. Numerical and Boundary Conditions for Flow Field Analysis

In this study, a total of four types of model: LBM, Standard k-ε model, low Re-type k-ε model, and LES, are used for flow field analysis in the benchmark test case shown in Fig. 1.

6.1. Lattice Boltzmann method

As for the LBM scheme with turbulence model, the D2Q9 (two-dimensional and nine velocities) model for 2D analysis and the D3Q19 (three-dimensional and nineteen velocities) model for 3D analysis were adopted with discretized velocity vector; for example, $c_0(0,0)$, $c_1(1,0)$, $c_2(0,1)$, $c_3(-1,0)$, $c_4(0,-1)$, $c_5(1,1)$, $c_6(-1,1)$, $c_7(-1,-1)$, and $c_8(1,-1)$ were used for the D2Q9 model. The BGK-based collision model was used.

Unsteady flow field analysis was carried out under the time step of fulfilling the CFL (Courant-Friedrichs-Lewy) condition. Physical time step for the simulation was set at $\Delta t = 1 \times 10^{-4}$ (s). In this LBM, we continued to execute the computations until the flow field characteristics became stable. As a result, the computation was conducted three times with nominal time constant τ_n (room volume/airflow rate) as the before-running calculation, and continuous calculations for nominal time constant τ_n were carried out two times for statistical analysis of turbulent characteristics. The numerical and boundary conditions for LBM are summarized in Table 1.

6.2. Standard k-ε model

The Navier-Stokes governing equations were discretized by a finite volume method and the QUICK scheme was used for the convection term, and a SIMPLE algorithm was used. Steady-state and two- and three-dimensional

Table 1. Numerical and boundary conditions for LBM

Lattice (voxel)	Regular square lattice: Total 5,084,856 (1,064(x) × 354(y) × 28(y), 3D cal.) (D3Q19 model) Total 751,184 (1,064(x) × 706(y), 2D cal.) (D2Q9 model)
Inflow boundary	$U_{in} = 0.455$ m/s, $TI = 0.04$, $l_{in} = (1/7)h$, $Re = 5{,}000$
Outflow boundary	Free slip
Wall treatment	No slip (bounce-back scheme)

Table 2. Numerical and boundary conditions for Standard k-ε model

EVM model	Standard k-ε model (Launder and Spalding)
Mesh	Structured grid: total 119,808 (96(x) × 48(y) × 26(z), 3D cal.) Structured grid: total 4,608 (96(x) × 48(y), 2D cal.)
Scheme	QUICK for advection term, SIMPLE algorithm
Inflow boundary	U_{in} = 0.455 m/s, $k_{in} = 3/2 \times (U_{in} \times 0.04)^2$, $\varepsilon_{in} = C_i^{3/4} \times k_{in}^{3/2}/l_{in}$, $C_i = 0.09$, $l_{in} = (1/7)h$
Outflow boundary	U_{out} = free slip, k_{out} = free slip, ε_{out} = free slip
Wall treatment	Velocity; Generalized log law

analyses were conducted. Generalized log law was adopted as wall function.

The numerical and boundary conditions for the Standard k-ε model are summarized in Table 2.

6.3. Low re-type k-ε model

The Navier-Stokes governing equations were also discretized by a finite volume method. The QUICK scheme was used for the convection term, and a SIMPLE algorithm was used. Steady-state and two- and three-dimensional analyses were conducted. To adopt the Abe-Nagano-Kondo model and to analyze the flow field in the boundary layer, the center of the computational cells closest to the wall surface should be at a non-dimensional distance (wall unit) of $y^+<1$, where $y^+ = u \times y_1/\nu$ and y_1 is the distance normal to the wall surface, ν is the kinematic viscosity, and $u^* = \sqrt{\tau_w/\rho}$ is the friction velocity. Here, ρ is the air density and τ_w is the wall shear stress. The numerical and boundary conditions for the low Re-type k-ε model are summarized in Table 3.

Table 3. Numerical and boundary conditions for low Re-type k-ε model

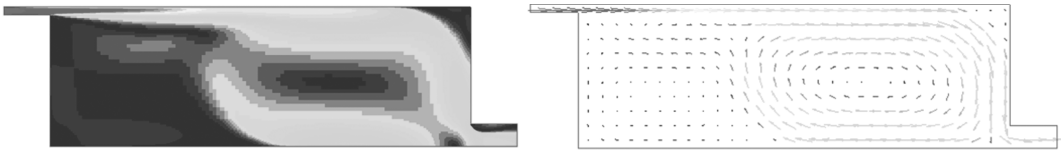
EVM model	low Re-type k-ε model (Abe-Nagano-Kondo model)
Mesh	Structured grid: total 4,428,648 (237(x) × 296(y) × 63(z), 3D cal.) Structured grid: total 127,512 (207(x) × 616(y), 2D cal.)
Scheme	QUICK for advection term, SIMPLE algorithm
Inflow boundary	U_{in} = 0.455 m/s, $k_{in} = 3/2 \times (U_{in} \times 0.04)^2$, $\varepsilon_{in} = C_i^{3/4} \times k_{in}^{3/2}/l_{in}$, $C_i = 0.09$, $l_{in} = (1/7)h$
Outflow boundary	U_{out} = free slip, k_{out} = free slip, ε_{out} = free slip
Wall treatment	Velocity; no slip

Table 4. Numerical and boundary conditions for LES

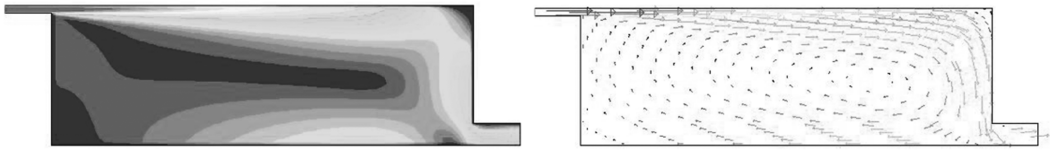
SGS model	Smagorinsky-Lilly model
Mesh	Structured grid: total 4,428,648 (237(x) × 296(y) × 63(z), 3D cal.)
Scheme	Space discretization: central difference Time discretization: 2nd -order Implicit
Inflow boundary	Vortex method (Generation of fluctuating inflow boundary condition)
Outflow boundary	Free slip
Wall treatment	No slip (Linear-power law)

6.4. LES with Smagorinsky-Lilly model

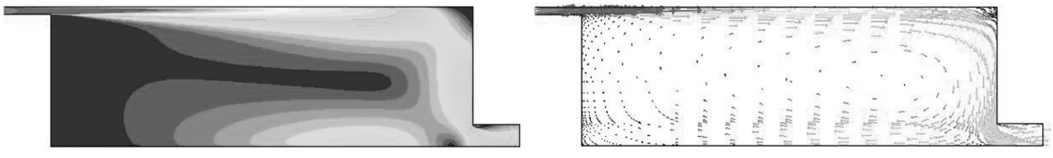
The special averaged (filtered) Navier-Stokes governing



(a) LBM with k-ε-type turbulence model



(b) Standard k-ε model



(c) Low re-type k-ε model

Figure 2. Velocity magnitude contours and velocity vector distributions for 2D case (left side fig., velocity magnitude; right side fig., velocity vector).

equations were solved. A second-order center difference scheme was used for the spatial derivatives. The second-order implicit scheme was used for the time advancement. In this study, Smagorinsky-Lilly model with Van Driest-type damping function was adopted.

$$D.F. = 1 - \exp\left(-\frac{y^+}{25}\right) \tag{16}$$

This damping function was incorporated into the $\overline{\Delta}$ of ν_{SGS} definition. Time-dependent fluctuating inflow boundary was generated by the vortex method.

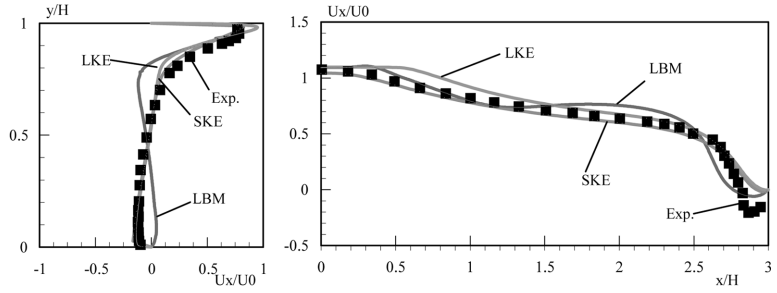
In this LES, computation was conducted three times for nominal time constant τ_n as the before-running calculation, and continuous calculations for the nominal time constant τ_n were carried out two times for statistical analysis of turbulent characteristics. The numerical and boundary conditions for LES are summarized in Table 4.

7. Results of Numerical Simulation for Flow Field Analysis

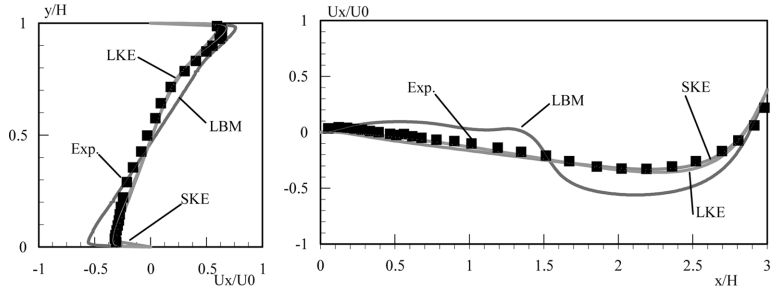
7.1. Results of 2-dimensional case

The benchmark simulation of the simple room cavity model shown in Fig. 1 was conducted in order to validate the prediction accuracy of LBM compared with that of the RANS model as a traditional CFD approach based on 2-dimensional analyses. The targeted problem is two-dimensional airflow at the central vertical section in the benchmark test domain. The target room geometry is a simple cuboid with one supply inlet slot and one exhaust outlet opening, and an incompressible fluid is assumed.

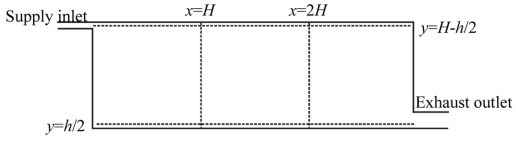
The velocity magnitude contours of the benchmark test case for the three models: LBM with turbulence model, Standard k-ε model and low Re-type k-ε model, are shown in Fig. 2. The velocity magnitude shown in Fig. 2 is the steady state simulation results of RANS model and the time-averaged value for LBM. In addition, in Fig. 2, the results of velocity vector distributions for the three models are also shown. As for LBM, unsteady and time-dependent simulations were carried out and hence instantaneous velocity vectors (time-averaged value between numerical time step in a precise sense) are shown in Fig. 2(1). The results of the Standard k-ε model and low Re k-ε model denote the ensemble-averaged velocity vector because of the steady-state simulation. With regard to the instantaneous velocity vector of LBM, the fluctuation of the vector seems to be low and a stable flow pattern in the test room was formed.



(a) $x=H$ (b) $y=H-h/2$



(c) $x=2H$ (d) $y=h/2$



(e) Supplemental figure of measured line

Figure 3. Velocity profiles at steady state.

The circulating flow attached to the ceiling and other side-wall surfaces was formed in the case of the Standard k-ε model and the low Re k-ε model. In the cases of LBM, the supply jet along the ceiling surface descended before reaching the opposite wall surface against the supply inlet opening. The result of LBM represented diffusive flow, especially in the prediction of supply jet. A clear difference of flow pattern at the left lower space in the model room was confirmed in the three models: Standard k-ε model, low Re k-ε model and LBM.

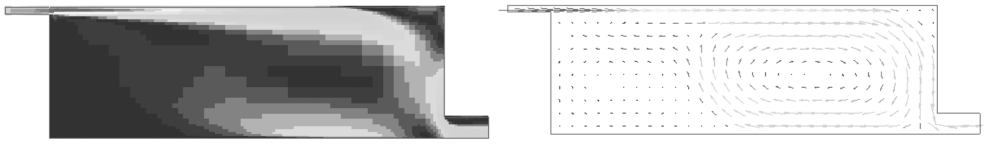
Fig. 3 shows comparisons between the results of these three models (LBM, Standard k-ε model and low Re-type k-ε model) in terms of velocity profiles at a steady state. In this study, the prediction results of the Standard k-ε model and low Re k-ε were reasonably consistent with experimental data measured by the LDV system and the prediction accuracy of LBM was relatively low compared with that of the RANS model.

7.2. Results of 3-dimensional cases

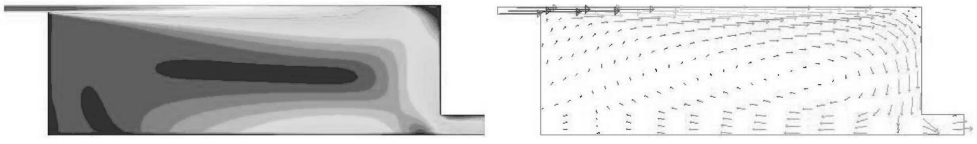
The time-averaged velocity magnitude contours of the benchmark test case for the four models: LBM with turbulence model, Standard k-ε model, low Re-type k-ε model and LES with Smagorinsky-Lilly model, are shown in Fig. 4. In addition, Fig. 4 shows the results of velocity vector distributions for the four turbulence models. For LBM and LES, unsteady and time-dependent simulations were carried out and hence instantaneous velocity vectors (time-averaged value between numerical time step in a precise sense for LBM) are shown in Fig. 4(1) and 4(4). The complicated instantaneous flow field (vector distribution) was confirmed in the case of LES because of the time-dependent fluctuating inflow boundary condition. On the other hand, the fluctuation of vector estimated by LBM seems to be low and a relatively stable flow pattern in the test room was formed compared with that of LES.

The tendency generating a circulating flow attached to the ceiling and the facing side-wall surfaces was similar to the results of 2-dimensional analyses and, especially with regard to the distributions of velocity magnitude for the Standard k-ε model and the low Re-type k-ε model, there were no significant differences between 2-dimensional analytical cases. Concerning the LBM, the result of 3-dimensional analyses seems to be consistent with the CFD results estimated by LES.

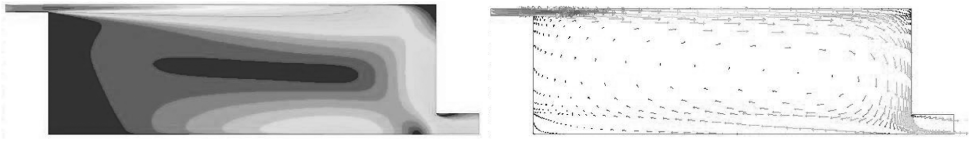
Fig. 5 shows comparisons between the results of the four models (LBM, Standard k-ε model, low Re-type k-ε model and LES) in terms of velocity profiles at a steady state. In this study, the prediction result of the Standard k-ε model and the low Re k-ε were reasonably consistent with experimental data, and these results seemed to be the same in 2-dimensional analyses. The prediction accuracies



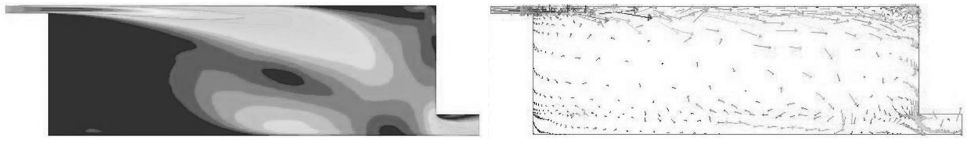
(a) LBM with k-ε-type turbulence model



(b) Standard k-ε model

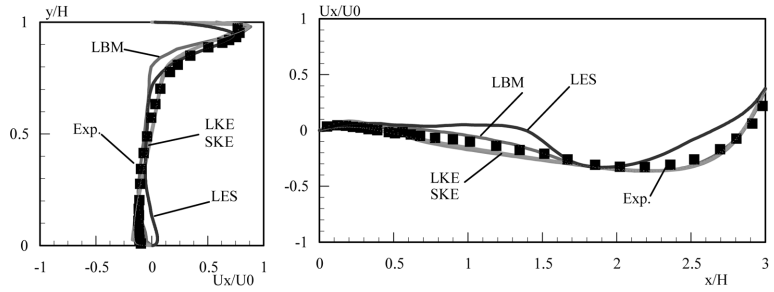


(c) low Re-type k-ε model

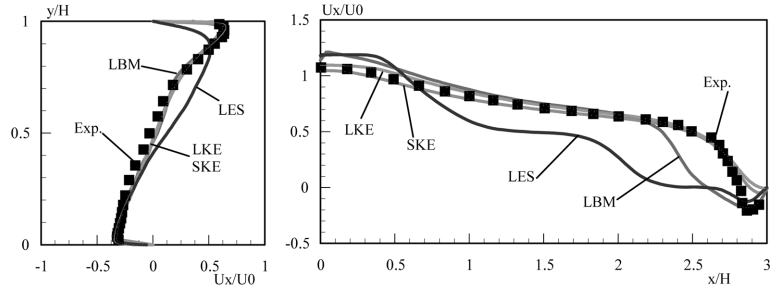


(d) LES

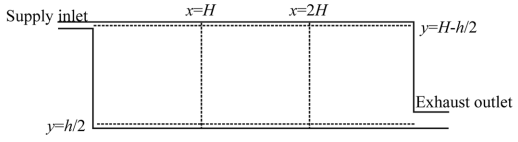
Figure 4. Velocity magnitude contours and velocity vector distributions for 3D case (left side fig., velocity magnitude; right side fig., velocity vector).



(a) $x=H$ (b) $y=H-h/2$



(c) $x=2H$ (d) $y=h/2$



(e) Supplemental figure of measured line

Figure 5. Velocity profiles at steady state.

of LBM in 3-dimensional analyses were improved and reasonably consistent with the experimental result compared with the results of 2-dimensional analyses of LBM. In this study, the prediction accuracy of LES was insufficient compared with those of other turbulence models, LBM and experiment. One of the reasons for this is the time-averaged operation of insufficient calculation time. Further discussion of the result of LES, for example, optimization of Cs, inflow boundary condition, grid design adopted, and so on, should be carried out.

Fig. 6 shows the results of vorticity distributions of the four models. The distribution of vorticity in Fig. 6 denotes the Z component (vorticity vector in the Z direction) on the X-Y plane. In the result of LES, locally high and non-uniform distribution of vorticity was observed.

8. Outline of Particle Dispersion Analysis Based on Lagrangian model

The particle motion is solved by the Lagrangian particle tracking method. In this study, steady flow field data-predicted LBM or CFD simulation was used and the effect of particle motion on the airflow was disregarded (one-way coupling approach) because of the low particle volume fraction; specifically, the Eulerian-Lagrangian particle tracking method was employed in this analysis. Eq. (17) indicates the particle dynamic equations for each particle transient momentum.

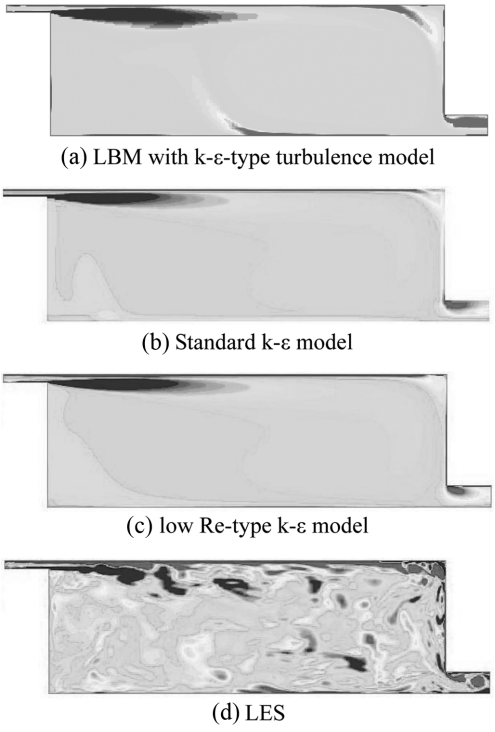
$$\frac{\partial u_p}{\partial t}=\frac{1}{\tau}(u+u'-u_p)+F_g \tag{17}$$

$$\frac{\partial x_p}{\partial t}=u_p \tag{18}$$

In this analysis, the second term on the right-hand side of Eq. (17) represents the drag force per unit particle mass, $\vec{u}$ is the fluid phase velocity, while $\vec{u}_p$ indicates particle velocity. τ denotes relaxation time of particles. x_p in Eq. (18) is the particle position. Here, drag force is expressed as follows:

$$\frac{1}{\tau}=F_D=\frac{18\mu}{\rho_p d_p^2}\cdot\frac{C_D Re_p}{24} \tag{19}$$

Here, μ is the molecular viscosity of the fluid, ρ is the air density, ρ_p is the density of the particle, and D_p is the particle diameter. Re_p is the Reynolds number defined using fluid viscosity μ as follows:



(a) LBM with k-ε-type turbulence model

(b) Standard k-ε model

(c) low Re-type k-ε model

(d) LES

Figure 6. Vorticity.

$$Re_p = \frac{\rho |u_p - u| d_p}{\mu} \tag{20}$$

C_D in Eq. (19) denotes the drag coefficient, which can be derived from Haider and Levenspiel (1989) as below:

$$C_D = a_1 + \frac{a_2}{Re_p} + \frac{a_3}{Re_p} \tag{21}$$

$\vec{F}_g$ indicates an additional acceleration term of gravitational effect and is presented in Eq. (22) and g is the gravitational acceleration.

$$F_g = \frac{(\rho_p - \rho)}{\rho_p} g \tag{22}$$

Concerning the particle tracking analyses for small particles, that is, submicron particles, the Brownian force and impact of turbulent diffusivity become important and are generally modeled as a Gaussian white noise random process and another random walk model. In this study, particles of 20 μm in diameter were assumed and hence the effects of turbulent fluctuations in the airflow and modeling of the Brownian force were disregarded for simplification, especially in order to emphasize the difference of prediction results of average flow field in the test case.

8.1. Numerical and boundary conditions for particle tracking analysis

The particle velocities and positions can be described by solving Eqs. (17) and (18). The Euler implicit discretization scheme was adopted for equation (17) and the second-order Lagrangian polynomial interpolation scheme was used for Eq. (18) to homologize the instantaneous particle positions and air-phase grid points.

The particles, which are assumed to have a spherical shape, have been launched at the opening of supply inlet (see Fig. 1). Here, a total of 10,000 particles were allocated uniformly. Particles of 20 μm in diameter and 1,000 kg/m^3 density were assumed. This study used a constant time step of $\Delta t = 1 \times 10^{-4}$ (s) and the maximum number of time steps was limited to 2×10^6 for each trajectory (= 20 sec). Concerning the wall surface treatment inside the room, perfect reflection in which no particle loss occurred on the wall surface was assumed.

9. Results of Particle Dispersion Analysis

The results of numerical analysis for particle dispersion in the target room space are shown in Fig. 7.

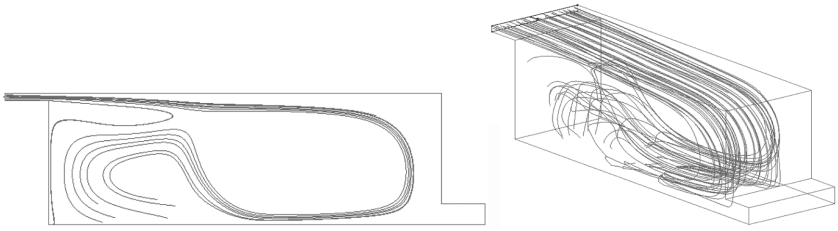
As shown in this figure, the spatial trajectory distributions of particles for D_p = 20 μm tended to follow a streamline of carrier airflow and gravitational settling effect seems to be fairly disregarded. In this analysis, the Brownian force and the effect of turbulence motion were not directly modeled and hence the differences of particle dispersion in three cases: LBM, Standard k-ε model and low Re-type k-ε model, were mainly caused by the difference of prediction results of the average flow pattern.

10. Conclusions

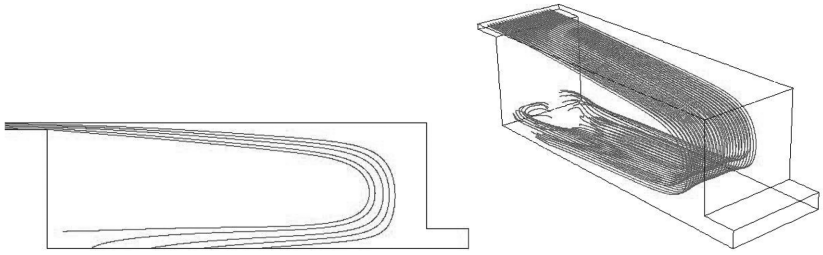
As the use of turbulence models in CFD increases, more sophisticated and universal models will be needed to simulate the phenomena that are observed in enclosed environments of high-rise buildings. The increasing complexity of applications to indoor environmental problems will require further development in engineering turbulence modeling and numerical methods.

In this paper, we have demonstrated the numerical procedure of Lattice Boltzmann method for flow field and particle dispersion analyses indoors, and have also shown the prediction results of flow pattern in a representative benchmark test case. Although the difference of prediction result in flow pattern was confirmed for the LBM-based scheme and LES and RANS models, the prediction results of LBM by 3-dimensional analyses were reasonably consistent with the experimental results and the prediction accuracy being similar to RANS and LES, as traditional CFD approaches, was confirmed. In other words, we confirmed that the LBM-based scheme has a good ability to predict flow field in an enclosed space.

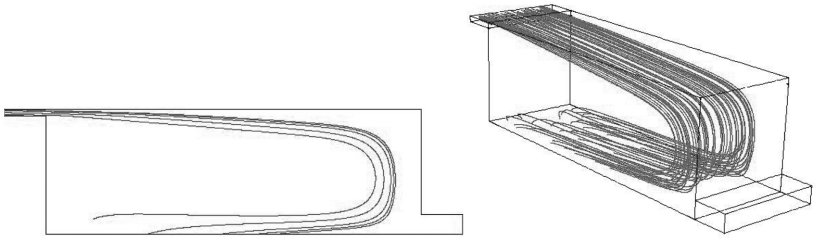
Furthermore, a hybrid-type coupling procedure of the LBM and the general dynamic equation of 20-μm-diameter particles based on a Lagrangian approach was presented and the results of particle tracking were also demonstrated. Airflow velocity played a dominant role in



(a) LBM with k-ε-type turbulence model



(b) Standard k-ε model



(c) low Re-type k-ε model

Figure 7. Particle path line of 20 μm diameter (left side fig., path line based on 2D flow field; right side fig., path line based on 3D flow field).

the particle motion in enclosed spaces and the improvement of prediction accuracy of airflow pattern will be crucial in this research field. Essentially, the LBM-based scheme has affinity with particle dynamic equations and, in the future, we will develop a more sophisticated procedure of integration between LEM and particle dynamic equations.

Acknowledgements

This research was partly supported by a Grant-in-Aid for Scientific Research (JSPS KAKENHI for Young Scientists (S), 21676005). The author would like to express special thanks to the funding source.

References

Abe, K., Nagano, Y., and Kondo, T. (1992) Numerical prediction of separating and reattaching flows with a modified low-Reynolds-number k-ε model. (1st int. Symp. Of Comp. Wind Eng., Tokyo), *J. Wind. Eng.*, 52, pp. 213~218.

Chen, S., and Doolen, G. D. (1998) Lattice boltzmann method for fluid flows. *Annual Review of Fluid Mechanics*, 30, pp. 329~364.

Frisch, U., Hasslacher, B., and Pomeau, Y. (1986) Lattice-gas automata for the Navier-stokes equation. *Physical Review Letters*, 56, pp. 1505~1508.

Grunau, D., Chen, S., and Eggert, K. (1993) A lattice Boltzmann model for multiphase fluid flows. *Physical Fluids*, A5, pp. 2557~2562.

He, X. Y., Zou, Q. S., Luo, J. S., and Dembo, M. (1997) Analytic solutions of simple flows and analysis of nonslip boundary conditions for the lattice Boltzmann BGK model. *J. Stat. Phys.*, 87, pp. 115~136.

Launder, B. E. and Spalding, D. B. (1972) Lectures in Mathematical Models of Turbulence. Academic Press, London, England

Lemaire A. D., Chen Q., Ewert M., Heikkinen J., Inard C., Moser A., Nielsen P. V., and Whittle, G. (1993) Room air and contaminant flow, evaluation of computational methods. Subtask-1 Summary Report, International Energy Agency, Annex 20, TNO Building and Construction Research, Delft, The Netherlands.

Lilly, D. K. (1966) On the application of the eddy viscosity concept in the inertial sub range of turbulence. *NCAR Manuscript*, 123.

Mizutani, K., Murakami, S., Kato, S., and Mochida, A. (1991) Indoor Air flow Analysis by LES, Study on the

optimization of Smagorinsky coefficient, Proceedings of Annual Conference of The Society of Heating, Air-Conditioning and Sanitary Engineers in Japan, pp. 901~904 (in Japanese).

Nielsen, P. V. (ed), Allard, F., Awbi, H. B., Davisdon, L., and Shalin, A. (2007) REHVA Guidebook 10, Computational Fluid Dynamics in Ventilation Design, REHVA.

Smagorinsky, J. (1963). General circulation experiments with the primitive equations I: The basic experiment. *Month. Weather Review*, 91, pp. 99~164.

Yu, D., Mei, R., Luo, L. S., and Shyy, W. (2003) Viscous flow computations with the method of lattice Boltzmann equation. *Progress in Aerospace Sciences*, 39, pp. 329~367.

Zhang, R., Shan, X., and Chen, H. (2006) Efficient kinetic method for fluid simulation beyond the Navier-Stokes equation. *Physical Review E*, 74, 046703.

Zhai, Z., Zhang, Z., Zhang, W., and Chen, Q. (2007) Evaluation of various turbulence models in predicting airflow and environments by CFD: Part 1-summary of prevalent turbulence models. *HVAC&R Research*, 13(6), pp. 853~870.

Zhang, Z., Zhang, W., Zhai, Z., and Chen, Q. (2007) Evaluation of various turbulence models in predicting airflow and environments by CFD: Part 2-comparison with experimental data from literature. *HVAC&R Research*, 13(6), pp. 871~886.

Bhatnagar, P. L., Gross, E. P., and Krook, M. (1954) A model for collision processes in gases. I. small amplitude processes in charged and neutral one-component systems. *Physical Review*, 94(3), p. 511~525.